BURIAL DEPTH OF THE RESERVOIRS OF HYDROGEN AT EQUATORIAL LATITUDES ON MARS

S. Maurice[1], O. Gasnault[1], W.C. Feldman[2], T.H. Prettyman[2], R.C. Elphic[2], D.J. Lawrence[2], [1]CESR/OMP, 9 av. Colonel Roche, 31400 Toulouse, France, sylvestre.maurice@cesr.fr, [2]LANL, Los Alamos, New Mexico

Introduction: At Mars, significant deposits of hydrogen have recently been observed by the GRS suite of instruments aboard Mars Odyssey [1,2,3]. Two energy ranges of neutron data are indeed very sensitive to hydrogen: epithermal (0.4 keV – 0.7 MeV) and fast (0.7 MeV – 10 MeV). This work will demonstrate that the comparison of these two energy ranges can be used to derive the burial depth of hydrogen at mid-latitudes. Assuming a simple stratigraphy of the Martian regolith, we calculate this burial depth and we show it is well correlated with topography.

Mid-latitude hydrogen deposits: We use about two years of continuous measurements. Data have been recently calibrated in an absolute manner, regardless of any reference to ground truth [4]. Count rates are transformed first into mass fraction of water equivalent hydrogen (M_{H2O}) [5]. Note that the convenient denomination "water equivalent hydrogen" (WEH) does not presume the actual molecular association of hydrogen [6,7]. Data points are mapped onto the planet; the surface resolution is ~600 km. When all uncertainties are folded together, estimates of M_{H2O} are accurate to less than about ±15%. Actually two values of M_{H2O} were determined from epithermal and fast neutron measurements. Based on epithermal data, values of M_{H2O} range from 2% to 15% between ±50° latitude. There are two large reservoirs of hydrogen at approximately antipodal longitudes. One is centered on Arabia Terra, longitude +25° E., near the equator. The other is just below the equator at longitude +185° E.

Stratigraphy of the Regolith: For this study, the vertical structure of the regolith is assumed a priori. It consists of two layers, whose elemental composition corresponds to that at the Pathfinder site [8]. The top layer, thickness *D*, is desiccated, with only 2% of WEH. The second layer extends infinitely, but with a higher mass fraction of WEH (parameter *H*). The two neutron energy ranges allow us to constrain the two parameters *D* and *H*. When *D*=0, the semi-infinite model yields an estimate of a maximum concentration of WEH.

Simulations of neutron production at the surface have been performed for a variety of *D* and *H* parameters, using the LANL-developed computer code MCNPX with appropriate cross sections and boundary conditions tailored to planetary applications. Neutrons are then transported to the spacecraft through a 16 g.cm^{-2} of atmosphere. Figure 1 summarizes these simulations. When D increases, M_{H2O} estimated from fast neutrons drops faster than M_{H2O} estimated from epithermal neutrons. Therefore, all simulations are on the right side of the *D*=0 line (semi-infinite model). Variations are most important for low values of *D*. When *D* is fixed, simulation points vary linearly with WEH. By construction, all lines cross at *H* = 2%.

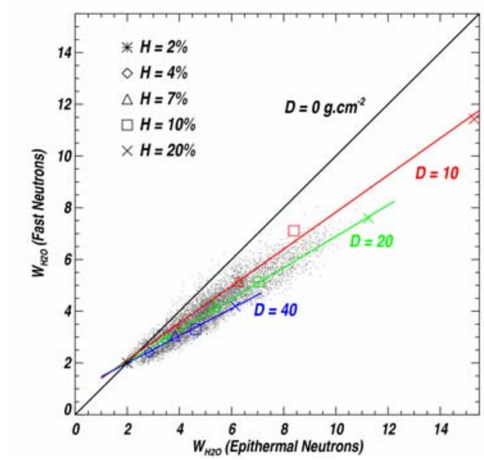

Figure 1: Simulations: Epithermal and fast neutrons estimates of M_{H2O} for different WEH concentrations and possible burial depth *D* under a desiccated layer. Data points are for 2°x2°) pixels equatorward of ±50° and limited to altitudes less than 5 km.

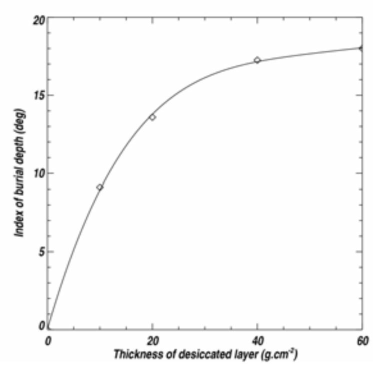

Figure 2: Relation between the burial depth parameter (α) and the thickness of the top layer (*D*).

Index of burial depth: Taking advantage of a linear dependence in WEH for a given value of *D*, we build an index of burial depth α, which is the angle

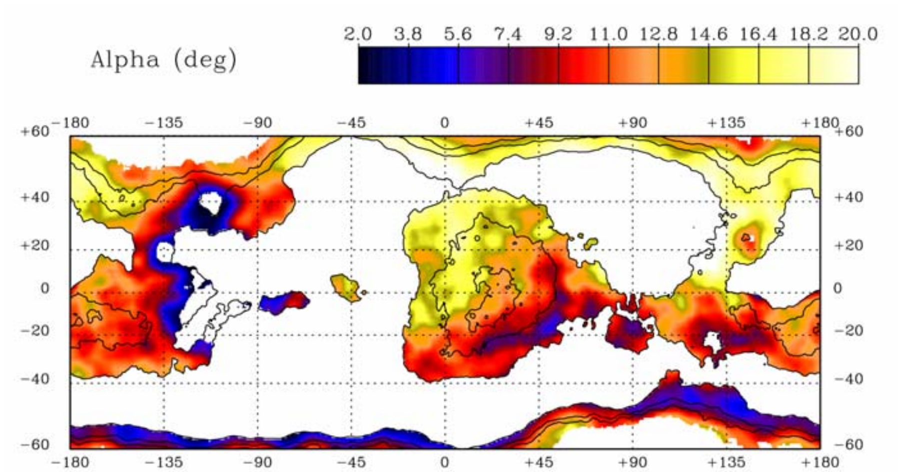

Figure 3: Index of burial depth for measured data points equatorward of ±60°, M_{H2O} larger than 5%, and altitude less than 5 km. Contours of M_{H2O} are for 5%, 7%, and 9%.

between the *D*=0 line and the line that passes through each data point and the 2% point. On Figure 1, it would be the angle between the red and black lines for data points falling along the *D*=10 g.cm^{-2} line. Therefore, there is a unique relation between *D* and α given figure 2. Above 40 g.cm^{-2}, the information on burial depth saturates since the difference between epithermal and fast neutron estimates of WEH gets too small and α levels off.

Measured data points are represented on Figure 1. for 2°x2° pixels equatorward of ±60°. They yield an angle between 0° and 20° with the semi-infinite model. Such data points are mapped onto the planet (figure 3) with the supplementary conditions that M_{H20} is larger than 5% (when WEH concentrations are too low, the accuracy of neutron count rates is not sufficient to determine a reliable burial depth) and altitudes are smaller than 5 km (fast neutron count rates at very high elevations have not yet been checked for proper calibration). The Arabia Terra reservoir is divided by a SW-NE line that follows the 0 km topography. Hydrogen deposits appear buried under more desiccated terrain on the West side of this frontier than on the East side. On the East side of the frontier (Terra Sabea), the concentration of WEH is between 5% and 7% and lies close to the surface. The antipodal reservoir has fewer variations. The westernmost connection (longitude +135° E) of this reservoir to the North Pole is buried at ~40 g.cm^{-2}, whereas its easternmost connection (longitude -135° E) is buried by less than 5 g.cm^{-2}.

Correlation with topography: Index of burial depth data points, plotted versus elevation (Figure 4) between -5 and +5 km (topography from MOLA) are smoothed at the same resolution as the neutron data. We observe an obvious correlation. It is much larger than possible calibration biases in the neutron data reduction. WEH at low elevation is buried under more desiccated regolith than at high elevation. This result relating the amount of dust that covers the surface of Mars to the depth of the seasonal temperature variations induced in the ground as a function its thermal properties [9] needs to be explored.

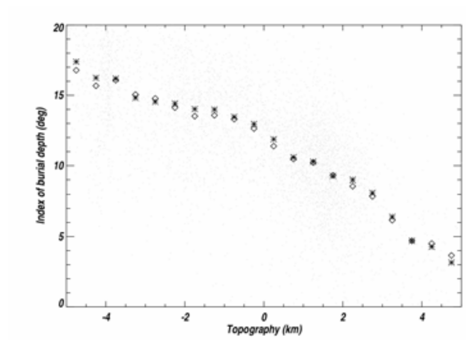

Figure 4: Index of burial depth for data points of Figure 3 as a function of topography. For 0.5 km bins, mean values (median) and median (star) are calculated.

References: [1] Boynton, W.V. (2002) *Science*, 297, 81. [2] Feldman, W.C. (2002) *Science*, 297, 75. [3] Mitrovanov, I. (2002) *Science*, 297, 78. [4] Prettyman, T. H. (2003) *JGR-Planets*, submitted. [5] Feldman, W.C., et al. (2003) *JGR-planets*, accepted. [6] Bish, D.L., et al. (2003) *Icarus*, in press. [7] Feldman , W.C., et al. (2004) LPSC XXXV. [8] Wänke, H., et al., *Space Sci. Rev.* (2001) 96, 317. [9]. [10] Mellon, M. T. (1997) *JGR-Planets*, 102, 25617.